



THE UNIVERSITY *of* EDINBURGH

Edinburgh Research Explorer

The MEF2 transcriptional target DMPK induces loss of sarcomere structure and cardiomyopathy

Citation for published version:

Damanafshan, A, Elzenaar, I, Samson-Couterie, B, van der Made, I, Bourajjaj, M, van den Hoogenhof, MMG, van Veen, HA, Picavet, DI, Beqqali, A, Ehler, E, De Windt, LJ, Pinto, YM & van Oort, RJ 2018, 'The MEF2 transcriptional target DMPK induces loss of sarcomere structure and cardiomyopathy', *Cardiovascular Research*, vol. 114, no. 11. <https://doi.org/10.1093/cvr/cvy091>

Digital Object Identifier (DOI):

[10.1093/cvr/cvy091](https://doi.org/10.1093/cvr/cvy091)

Link:

[Link to publication record in Edinburgh Research Explorer](#)

Document Version:

Peer reviewed version

Published In:

Cardiovascular Research

General rights

Copyright for the publications made accessible via the Edinburgh Research Explorer is retained by the author(s) and / or other copyright owners and it is a condition of accessing these publications that users recognise and abide by the legal requirements associated with these rights.

Take down policy

The University of Edinburgh has made every reasonable effort to ensure that Edinburgh Research Explorer content complies with UK legislation. If you believe that the public display of this file breaches copyright please contact openaccess@ed.ac.uk providing details, and we will remove access to the work immediately and investigate your claim.



The MEF2 transcriptional target DMPK induces loss of sarcomere structure and cardiomyopathy

Amin Damanafshan^{1*}, Ies Elzenaar^{1*}, Benoit Samson-Couterie¹, Ingeborg van der Made¹, Meriem Bourajjaj², Maarten M. van den Hoogenhof¹, Henk A. van Veen³, Daisy I. Picavet³, Abdelaziz Beqqali¹, Elisabeth Ehler⁴, Leon J. De Windt², Yigal M. Pinto¹,
Ralph J. van Oort¹

¹*Department of Experimental Cardiology, Amsterdam Cardiovascular Sciences, Academic Medical Center, Amsterdam, The Netherlands.*

²*Department of Cardiology, Maastricht University, Maastricht, The Netherlands.*

³*Electron Microscopy Centre Amsterdam, Department of Medical Biology, Academic Medical Center, Amsterdam, The Netherlands.*

⁴*Cardiovascular Division, King's College, London, United Kingdom.*

* Authors contributed equally

The authors have declared that no conflict of interest exists.

Address correspondence to:

Dr. Ralph J. van Oort, Department of Experimental Cardiology, Amsterdam Cardiovascular Sciences, Academic Medical Center, Meibergdreef 15, 1105 AZ, Amsterdam, The Netherlands, Tel.: +31-20-5664681; e-mail: r.j.vanoort@amc.uva.nl

Word count: 8095

ABSTRACT

Aim: The pathology of heart failure is characterized by poorly contracting and dilated ventricles. At the cellular level, this is associated with lengthening of individual cardiomyocytes and loss of sarcomeres. While it is known that the transcription factor myocyte enhancer factor -2 (MEF2) is involved in this cardiomyocyte remodeling, the underlying mechanism remains to be elucidated. Here, we aim to mechanistically link MEF2 target genes with loss of sarcomeres during cardiomyocyte remodeling.

Methods and Results: Neonatal rat cardiomyocytes overexpressing MEF2 elongated and lost their sarcomeric structure. We identified myotonic dystrophy protein kinase (DMPK) as direct MEF2 target gene involved in this process. Adenoviral overexpression of DMPK E, the isoform upregulated in heart failure, resulted in severe loss of sarcomeres *in vitro* and transgenic mice overexpressing DMPK E displayed disruption of sarcomere structure and cardiomyopathy *in vivo*. Moreover, we found a decreased expression of sarcomeric genes following DMPK E gain-of-function. These genes are targets of the transcription factor serum response factor (SRF) and we found that DMPK E acts as inhibitor of SRF transcriptional activity.

Conclusions: Our data indicate that MEF2-induced loss of sarcomeres is mediated by DMPK via a decrease in sarcomeric gene expression by interfering with SRF transcriptional activity. Together, these results demonstrate an unexpected role for DMPK as a direct mediator of adverse cardiomyocyte remodeling and heart failure.

INTRODUCTION

The heart responds to stress or injury by hypertrophic growth, an initially compensatory structural remodeling, which often progresses to cardiac wall thinning, chamber dilation and heart failure. Although this transition from cardiac hypertrophy to heart failure has been associated with lengthening of individual cardiomyocytes and loss of sarcomeres¹⁻³, the mechanisms underlying these changes in cardiomyocyte structure remain to be elucidated. Increasing evidence, however, suggests a role for the transcription factor myocyte enhancer factor-2 (MEF2) as trigger for this adverse structural remodeling of cardiomyocytes^{4,5}.

MEF2 was originally identified as a muscle-specific DNA binding factor that recognizes conserved A/T-rich elements in enhancers of numerous muscle-specific genes⁶. To date, four MEF2 genes, *mef2a*, *-b*, *-c*, and *-d*, have been characterized in vertebrates, with an expression pattern and function that extends beyond striated muscle. MEF2 transcription factors share high homology in an amino-terminal MADS (MCM1, Agamous, Deficiens, and Serum response factor) box and an adjacent MEF2-specific domain, which together mediate dimerization and binding to the consensus DNA sequence CTA(AT)₄TA(G/A)^{7, 8}. MEF2 has been implicated in the embryonic development of cardiac, skeletal, and smooth muscle, and in postnatal heart disease⁹.

MEF2 has initially been postulated to play a role in the development of cardiac hypertrophy, as its activity is upregulated by several pro-hypertrophic signaling cascades, including calcineurin, calcium/calmodulin-dependent protein kinase, and mitogen-activated protein kinase pathways¹⁰. We and others, however, have demonstrated that overexpression of either MEF2A, MEF2C or MEF2D in the postnatal heart minimally triggers the classical hypertrophic growth response, but rather induces dilated cardiomyopathy^{4, 5, 11}. At the cellular level, MEF2 activation resulted in elongation of cardiomyocytes and possibly disorganization of sarcomere structure^{4, 5}. Conversely, *in vivo* inhibition of MEF2 activity did not prevent

calcineurin-induced cardiac hypertrophy, but profoundly reduced cardiac dilation and improved contractility⁴. Furthermore, cardiac specific deletion of MEF2D protected against pressure overload-induced cardiac remodeling and dysfunction¹¹. Overall, these results imply that MEF2 activates a gene program triggering cardiac dilation and loss of contractility. However, the therapeutic value of targeting MEF2 to prevent cardiac dilation and dysfunction in heart failure has been challenged, since inhibition of all MEF2 activity leads to mitochondrial dysfunction accelerating heart failure development¹².

Since previous results indicate that MEF2 regulates expression of genes controlling both the adaptive response of the heart to stress as well as genes involved in the maladaptive structural remodeling during heart failure development, we aimed to identify MEF2 target genes responsible for the adverse cardiomyocyte remodeling associated with cardiomyopathy. Here, we describe myotonic dystrophy protein kinase (DMPK) as transcriptional target of MEF2 involved in loss of sarcomere structure in heart failure.

METHODS

Detailed experimental protocols are in the Supplementary material online.

Recombinant viruses. Recombinant adenoviruses were generated as described previously⁴. Lentiviruses were generated by cloning cDNA inserts into pLenti-C-GFP (Origine, PS100065) or pLenti-C-tRFP (Origine, PS100074) and co-transfection with third-generation lentiviral packaging plasmids pMDLg/pRRE (Addgene, 12251), pRSV-Rev (Addgene, 12253) and the pMD2.G envelope plasmid (Addgene, 12259) into HEK293T cells.

Cell culture and transient transfection assays. Neonatal rat ventricular cardiomyocytes (NRCM) were isolated from 1-3 days old Wistar rats and cultured as described before⁴. Low passage HEK293T cells were cultured in DMEM supplemented with 10% FBS. NkL-TAg cells were cultured as described previously¹³. NkL-TAg cells were transiently transfected using FuGENE 6 reagent (Roche). NRCM were transfected using Lipofectamin 2000 (Invitrogen).

Generation of stable cardiac cell lines. Two independent double stable NkL-TAg cell lines (TR1-194 and TR4-39), inducibly expressing the constitutively active MEF2VP16 (caMEF2), were generated using the T-REX system (Invitrogen).

Gene expression profiling. TR1-194 and TR4-39 clones were maintained in parallel cultures, immortalized by overnight AdCre infection, cultured for an additional 3 days in serum-free media either in the presence or absence of 24 h Dox-treatment. Three corresponding cultures were pooled, total RNA extracted using TRIzol (Invitrogen) and cleaned with Qiagen RNeasy Mini Kits (Qiagen). RNA quantity was measured with a NanoDrop® ND-1000 UV-Vis Spectrophotometer (Wilmington), and RNA quality was monitored using an Agilent 2100 bioanalyzer. Gene

expression profiling was performed using Agilent 44k mouse whole genome microarray slides following the manufacturer's protocol.

Immunofluorescence and confocal microscopy. Cultured cardiomyocytes were fixed for 10 min in 4% paraformaldehyde and permeabilized with 0.2% Triton X-100 in PBS for 5 minutes. Primary and secondary antibodies were diluted using 1% BSA in TBS and incubations were carried out at room temperature for 1 hour. Cells were washed 3 times with PBS for 5 minutes, mounted with coverslips in 0.1 M Tris-HCl (pH 9.5)-glycerol (3:7) including 50 mg/ml *n*-propylgallate as anti-fading reagent, and analyzed by confocal microscopy using a Zeiss LSM 510 META instrument or a Leica TCS SP8 X / DMI6000 inverted confocal microscope.

Histology. Hearts were fixed in 4% paraformaldehyde, dehydrated in graded alcohol solutions and Histo-Clear and embedded in paraffin. Sections were stained with hematoxylin and eosin (H&E), or picosirius red to determine the amount of fibrosis. For immunofluorescence, primary antibodies against α -actinin (A7811, Sigma, 1:500) and SRF (sc-335, Santa Cruz, 1:250) were used.

Electron microscopy. Left ventricular tissue was prefixed in 1% glutaraldehyde, 4% paraformaldehyde in 0.1 M sodium cacodylate (Merck) and processed for electron microscopy. Images were acquired with a FEI technai 12 transmission electron microscope.

Western blot analysis. Protein lysates from cells or cardiac tissue were separated by electrophoresis, transferred to polyvinylidene difluoride membranes and processed for chemiluminescent detection. Chemiluminescence was captured by the ImageQuant LAS-4000.

Reverse-transcription and Real-Time Polymerase Chain Reaction. Total RNA was isolated from the indicated cell types or tissue using TRIzol reagent (Invitrogen). One μg of RNA isolated from flash-frozen apex was reverse-transcribed using Oligo(dT) primers and Superscript II reverse transcriptase (Invitrogen). PCR amplification was performed in a total reaction volume of 50 μl and PCR products were resolved by agarose gel electrophoresis. Real-time PCR was performed in 384-well plates using SYBR Green I master solution (Roche) and the LightCycler 480 (Roche).

Chromatin immunoprecipitation. Chromatin immunoprecipitation was carried out using the Upstate Biotechnology ChIP assay kit.

Animal studies. Cardiac specific DMPK E and DMPK E (K100A) overexpression mice were generated by subcloning DMPK E and DMPK E (K100A) cDNA into an αMHC transgenic vector. The transgenic vectors were injected into the pronuclei of fertilized FVB oocytes, which were transferred to pseudopregnant recipients. Transverse Aortic Constriction (TAC) and echocardiography were performed as described previously¹². For echocardiography measurement, mice were anesthetized using 1.5% isoflurane mixed with 95% O_2 . For TAC surgeries, 8 weeks old male C57/BL6 mice (Harlan) were anesthetized with 2% isoflurane and sacrificed 12 weeks after surgery by cervical dislocation in 2% isoflurane. Animal studies conformed to the Directive 2010/63/EU of the European Parliament, and were approved by the Animal Experimental Committee of the Academic Medical Center, University of Amsterdam.

Statistics. The results are presented as means \pm SEM. Statistical analyses were performed using INSTAT 3.0 and GraphPad Prism7 software (GraphPad, San Diego) and an unpaired 2-tailed Student's t-test, or one way ANOVA followed by Tukey's post-test. Statistical significance was accepted at a P value < 0.05 .

RESULTS

Activation of MEF2 leads to elongation and loss of sarcomeres in cultured cardiomyocytes

To address the role of MEF2 in structural remodeling of cardiomyocytes, we generated adenoviruses expressing either MEF2A (AdMEF2A) or the constitutively active MEF2VP16 (AdcaMEF2). Isolated neonatal rat cardiomyocytes (NRCM) were infected with AdMEF2A, AdcaMEF2 and control AdGFP for 48 hours, fixed and stained for the sarcomeric proteins titin, at both the M-band (titin M8) and Z-disc (titin T12), α -actinin (Z-disk) and myomesin (M-band), (Fig. 1A and B). First, we determined the ratio of the length of the major and minor axis of cells, as a measure of cellular elongation. AdGFP infected cardiomyocytes had a ratio of 2.57 ± 0.16 , while AdMEF2A and AdcaMEF2 infected cells displayed a 2- and 3 fold increase in major to minor axis ratios (5.20 ± 0.50 and 7.70 ± 0.77 , respectively; $P < 0.05$) compared to AdGFP-infected cells (Fig. 1C). Next, we analyzed the MEF2-induced sarcomere phenotype. Non-infected and AdGFP infected NRCM displayed a regular pattern of sarcomere staining, with a regular spacing between the M-band and the Z-disc. In contrast, quantification of myofibrillar structure score showed a dramatic loss of sarcomeres in AdMEF2A and AdcaMEF2 infected NRCM (Fig. 1D). Combined, these data demonstrate that MEF2 transcriptional activity in cultured cardiomyocytes promotes elongation of cardiomyocytes, accompanied by loss of sarcomere structure.

MEF2 activates cardiac genes involved in cardiomyocyte structure

To reveal the potential mechanisms underlying the structural cardiomyocyte changes induced by MEF2 transcriptional activity, we screened for MEF2 target genes. For this, we generated a

cellular system to inducibly activate MEF2 in NkL-TAg cells, a previously described ventricular muscle cell line¹³ (Fig. S1 and Fig. 2A). We obtained 8 double-stable cell lines, which only expressed caMEF2 after doxycyclin (Dox) stimulation, as demonstrated by Western blotting using an antibody against VP16 (Fig. S1B) and by immunofluorescent staining (Fig. S1C). To control for cell-based variations, we selected 2 TR-caMEF2 clones (TR1-194 and TR4-39) for further analysis. Both clones were transiently transfected with 3xMEF2 luc, immortalized with AdCre infection¹³, cultured for 72 hours in serum free media to allow to adopt a ventricular muscle cell fate, and exposed to Dox for varying periods to establish at which time-course elevated MEF2 transcriptional activity was evident. In both clones, an approximate 5-fold increase of MEF2 transcriptional activity was evident at 8 h, compared to TR1-194 and TR4-39 clones cultured in the absence of Dox (Fig. 2B). After 24 h Dox exposure, both clones demonstrated an approximate 10-fold increase in MEF2 transcriptional activity (Fig. 2B). Both TR1-194 and TR4-39 cell lines elongated after Cre-induced immortalization and Dox stimulation (Fig. S1C). So, we established a novel system that allows inducible activation of MEF2 transcriptional activity in ventricular muscle cells by addition of doxycyclin to the culture medium.

Both inducible caMEF2 ventricular myocyte cell lines were used for a genome-wide microarray analysis to identify the earliest gene pattern regulated by MEF2. After cells were immortalized by AdCre infection¹³, cultured in serum free medium for 72 hours and cultured for an additional 24 hours in the absence or presence of Dox, we found 75 genes to be differentially expressed in both TR1-194 and TR4-39 cells with a fold change in expression ≥ 2 ($P < 0.01$) after Dox stimulation (Supplemental table). Gene ontology classifications revealed an overrepresentation of genes in several subclasses, among which cell-matrix adhesion and cytoskeletal remodeling (Fig. 2C). Another gene class differentially regulated by MEF2 included genes involved in energy metabolism and mitochondrial energy production (Fig. 2C), which is in line with previous reports indicating a direct or indirect role for MEF2 to control cardiac energy production^{12, 14, 15}. We picked 10 genes and verified differential expression by RT-PCR (Fig. 2D)

and QPCR analysis (Fig. 2E). For example, transcripts for *integrin alpha-7* (*Itga7*), *nexilin* (*Nexn*), *connective tissue growth factor* (*Ctgf*), *regulatory myosin light chain 9* (*Myl9*), *myotonic dystrophy protein kinase* (*Dmpk*), *sarcoglycan alpha* (*Sgca*) and *sarcoglycan beta* (*Sgcb*) were upregulated upon caMEF2 expression in TR1-194 and TR4-39 clones (Fig. 2D and E). In contrast, transcripts for *integrin beta 4* (*Itgb4*), *glutathione S-transferase alpha 1* (*Gsta1*) and *mucin 5* (*Muc5b*) were downregulated. Combined, these data demonstrate that MEF2 activates subsets of genes primarily involved in cardiomyocyte structure and energy metabolism.

DMPK is a MEF2 target gene required for loss of sarcomere structure

Of all genes found to be upregulated by MEF2 activation, DMPK was of specific interest. DMPK is a kinase related to the Rho family of kinases and has been implicated in disruption of sarcomere structure in earlier *in vitro* studies^{16, 17}. Also, DMPK protein levels are increased in human failing hearts¹⁸. To verify that DMPK represents a direct transcriptional target of MEF2, rat, mouse and human orthologs were aligned and analyzed for conserved MEF2 binding sites. One conserved MEF2 binding sequence (CTAAATTTAA) was detected 513 bp upstream of the transcriptional start site of the rat *Dmpk* gene (Fig. 3A). We performed ChIP analysis to determine whether MEF2 binds to this A/T rich motif (Fig. 3B). Chromatin was immunoprecipitated from rat neonatal cardiomyocytes infected with either AdGFP or AdMEF2A, using antibodies directed against MEF2 and acetylated histone H3. No antibody immunoprecipitates were used as negative control. PCR amplification of the immunoprecipitated material using primers flanking the MEF2 site, demonstrated MEF2 binding to the *Dmpk* promoter in cardiomyocytes infected with the MEF2A expressing adenovirus (Fig. 3B).

In order to assess the potential role of DMPK in MEF2-induced cardiomyocyte remodeling, we evaluated the effect of DMPK siRNA-mediated knockdown during this remodeling process. As determined by Western blotting, we established significant knockdown of DMPK expression levels by transfecting cardiomyocytes with siRNAs directed against DMPK

(Fig. 3C). Infection with AdMEF2A and especially AdcaMEF2 enhanced DMPK protein levels in cardiomyocytes pre-transfected with control siRNA. This increase in expression, however, was inhibited in cardiomyocytes pre-transfected with siRNA targeting DMPK (Fig. 3C). Next, we investigated the effect of DMPK inhibition on MEF2-induced structural remodeling of cardiomyocytes. Pre-transfection with control siRNA had no effect on cellular morphology. MEF2 activation induced elongation and loss of sarcomere structure in cardiomyocytes transfected with control siRNA (Fig. 3D). Cardiomyocytes pre-transfected with DMPK siRNA, however, showed a clear attenuation of characteristic MEF2-induced sarcomeric degeneration (Fig. 3D). Conclusively, DMPK is a direct cardiac MEF2 target gene and promotes loss of sarcomere structure.

DMPK E is increased in heart failure and is sufficient to induce loss of sarcomere structure

To assess a possible role for DMPK in loss of sarcomere structure in the intact heart, we analyzed DMPK protein and mRNA levels in hearts from mice subjected to transverse aortic constriction (TAC) or sham surgery (Fig. S3). Western blot analysis displayed a significant increase in DMPK protein levels only in failing mouse hearts (ejection fraction (EF) <35%) and not in hearts from mice with cardiac hypertrophy and preserved cardiac function (Fig. 4A and B). DMPK RNA is subject to extensive alternative splicing, giving rise to 6 major (DMPK A-F) and several minor DMPK isoforms¹⁹. Alternative splicing events in the C-terminus (mainly resulting in in- or exclusion of exons 13 and 14) are likely to be the main determinants of DMPK functional variability, since they give rise to DMPK isoforms with long C-termini (DMPK A-D) that can anchor into membranes of mitochondria or the sarcoplasmic reticulum, or to smaller isoforms (DMPK E and F) with a cytosolic localization due to lack of the C-terminal extension²⁰. So, we first determined the expression levels of different DMPK isoforms in failing mouse hearts and sham control hearts by RT-PCR using primers spanning exons 13 and 14 (Fig. 4C).

Interestingly, mainly the DMPK E isoform, resulting from skipping of both exon 13 and 14, was upregulated in failing hearts. Indeed, quantitative PCR (QPCR) specifically for this isoform showed a significant increase in DMPK E mRNA in failing hearts (Fig. 4D). Interestingly, RT-PCR and QPCR analysis in NRCM showed that it is particularly the DMPK E isoform that is upregulated upon MEF2 activation (Fig. S3A-C). Western blot analysis demonstrates that both the MEF2A and the caMEF2 construct increase DMPK protein levels (Fig. S3D).

To further identify a role for DMPK E in sarcomere degeneration, we generated adenoviruses expressing either DMPK E (AdDMPK E) or a kinase dead mutant DMPK E (AdDMPK E (K100A); Fig. 4E)²⁰ and used these viruses, along with a GFP control virus, to infect isolated cardiomyocytes. Immunostaining for α -actinin and quantification of myofibrillar structure scores demonstrated a clear loss of sarcomere structure in NRCM 48 hours after infection with AdDMPK E, but not with AdDMPK E (K100A) or AdGFP (Fig. 4F and G). Overall, these data demonstrate that expression of DMPK E is increased in failing hearts and that overexpression of this specific isoform is sufficient to induce loss of sarcomeres in isolated cardiomyocytes. Furthermore, the DMPK E-induced effect on sarcomere structure requires DMPK E to be enzymatically active, indicating the involvement of one or more downstream phosphorylation events.

DMPK E inhibits SRF transcriptional activity

Loss of sarcomeres can be induced by both an increase in sarcomere protein degradation and a decrease in sarcomere generation. To test this, we performed QPCR analysis for several sarcomeric genes, including *α -actinin* (Actn2), *titin* (Ttn), synaptopodin 2-like (Chapb), skeletal alpha actin (Acta1) and *myosin light chain 2* (Myl2) on RNA isolated from NRCM infected with AdGFP, AdDMPK E, AdDMPK E (K100A) and AdcaMEF2 (Fig. 5A). Strikingly, the expression of all sarcomeric genes tested was dramatically reduced in NRCM infected with AdDMPK E compared to cells infected with AdGFP or AdDMPK E (K100A). A smaller, but still significant,

decrease in *Actn2*, *Ttn*, *Acta1* and *Myl2* mRNA was also observed in NRCM infected with MEF2 virus, which is in line with DMPK being the MEF2 target involved in sarcomere loss (Fig. 3D). The expression level of cardiac *NK2 homeobox 5* (*Nkx2.5*) was similar in all conditions (Fig. 5A), assuring an equal number of cardiomyocytes after infection with the different viruses. So, DMPK E-induced loss of sarcomeres is caused by a decrease in transcription of sarcomeric genes.

Interestingly, among the few known phosphorylation targets of DMPK is serum response factor (SRF), a transcription factor controlling cardiac sarcomere gene expression²¹. To check whether DMPK E inhibits SRF transcriptional activity in our cardiomyocytes, we transfected NRCM with the SM22 luc reporter for SRF activity together with or without the SRF cofactor myocardin (*Myocd*)²². At baseline, luciferase signal in AdDMPK E infected NRCM was significantly lower than in AdGFP or AdDMPK E (K100A) infected cells. Furthermore, co-transfection with *Myocd* resulted in a significant increase in luciferase signal, indicating enhanced SRF activity, in cells infected with AdGFP and AdDMPK E (K100A), but not in cells infected with AdDMPK E (Fig. 5B). These data demonstrate that DMPK E inhibits SRF transcriptional activity.

DMPK is known to phosphorylate threonine 159 and possibly serine 162 in the MADS box, the DNA binding domain of SRF²¹. These phosphorylation events have been described to weaken the binding of SRF to the promoter regions of sarcomeric genes, thereby decreasing their expression levels^{23, 24}. Therefore, we explored the potential effects of DMPK E on cellular localization of SRF by immunostainings (Fig. 5C and D). NRCM infected with AdGFP or AdDMPK E (K100A) displayed an expected nuclear localization of SRF. In contrast, AdDMPK E infected NRCM showed a significant increase in translocation of SRF from the nucleus (Fig. 5C and D). Next, we compared the effect of the full-length DMPK A isoform and the cytosolic DMPK E isoform on both sarcomere disruption and SRF translocation in NRCM (Fig. S4). NRCM transduced with DMPK E showed a much larger sarcomere disorganization and more SRF translocation than NRCM transduced with DMPK A, indicating that it is the cytosolic variant of

DMPK that induces SRF translocation and thereby sarcomere disruption. Combined, DMPK E decreases transcription of sarcomeric genes, due to an SRF nucleo-cytoplasmic translocation event and concomitant inhibition of SRF transcriptional activity.

DMPK E-induced loss of sarcomere structure requires phosphorylation of SRF

DMPK is known to phosphorylate SRF at threonine 159 and serine 162²¹. To investigate whether phosphorylation of SRF is the main mechanistic driver for DMPK E-induced sarcomere degeneration, we generated lentiviruses expressing either wildtype SRF (SRF-WT), a nonphosphorylatable mutant SRF in which the serine and threonine sites have been mutated to alanine (SRF-TASA), and a phosphomimic mutant in which these sites have been mutated to aspartic acid (SRF-TDSD). We then co-infected NRCM with these viruses and with either AdGFP or AdDMPK E, and assessed the amount of nuclear SRF (Fig. 6A and B). Quantification of the percentage of nuclear SRF showed that the phosphomimic TDSD SRF mutant translocates out of the nucleus independent of DMPK E. Furthermore, the SRF-TASA mutant remains located in the nucleus even in the presence of DMPK E.

Since the unphosphorylatable TASA SRF mutant remains located in the nucleus, we investigated the effect of SRF-TASA overexpression on AdDMPK E-induced loss of sarcomeres (Fig. 6C). Quantification of the myofibrillar structure showed that NRCM infected with lenti-SRF-TASA were protected from DMPK E-induced sarcomere disruption (Fig. 6D). Combined, these results demonstrate that DMPK E-induced loss of sarcomeres requires phosphorylation of SRF.

DMPK E activity induces loss of cardiac sarcomere structure and cardiomyopathy in mice

Our *in vitro* findings indicate that DMPK is required for MEF2-induced sarcomere loss and that DMPK E is sufficient to induce loss of sarcomere structure. To define whether DMPK E is also sufficient to induce structural remodeling of the heart, we generated mice expressing either DMPK E or DMPK E (K100A) under control of the cardiac specific alpha myosin heavy chain

promoter. For both constructs we obtained 2 independent transgenic lines, designated DMPK E lines 1 and 2 and DMPK E (K100A) lines 1 and 2, with matched levels of overexpression as determined by Western blot analysis (Fig. 7A). QPCR analysis indicates that DMPK E mRNA levels in DMPK E (K100A) hearts are higher than in the DMPK E mouse lines (Fig. 7B). DMPK E mRNA levels in DMPK E line 2 hearts are lower compared to DMPK E line 1 hearts (Fig. 7B). So, hearts of control DMPK E (K100A) mice express equal or slightly higher amounts of DMPK E protein compared to DMPK E mice. However, DMPK E (K100A) mice lack DMPK kinase activity, as depicted by the absence of DMPK autophosphorylation (no higher DMPK protein product on Western blot; Fig. 7A).

Strikingly, survival rate was significantly reduced in both DMPK E lines, with mortality of 70% and 20% in 7-month-old DMPK E line 1 and DMPK E line 2 mice, respectively, compared to no mortality in wildtype (WT) or both DMPK E (K100A) mouse lines (Fig. 7C). Hearts from 8-month-old DMPK E (K100A) mice displayed no structural abnormalities compared to age matched WT hearts (Fig. 7D). Hearts from DMPK E transgenic mice, however, showed clear signs of cardiomyopathy, with dilation of both ventricles and occasional enlargement of atria, at an age of 5 and 8 months for lines 1 and 2, respectively (Fig. 7D). Next, we performed echocardiographic analysis of WT, DMPK E and DMPK E (K100A) mice to assess cardiac dimensions and function over time. Although we did not find any differences in wall thickness or ventricular diameter within 6 months of age, DMPK E transgenic mice displayed a clear loss of cardiac function compared to WT and DMPK E (K100A) control mice (Fig. S5A). To assess the amount of fibrosis, we performed Sirius Red stainings, which showed a significant increase in fibrotic cardiac tissue in DMPK E mice (Fig. S5B). To investigate whether the DMPK E phenotype could be due to increased cardiomyocyte death, we assessed the extent of cardiomyocyte apoptosis by TUNEL staining (Fig. S6). These data demonstrated that there is no increase in cardiomyocyte apoptosis in DMPK E transgenic mice. The cardiomyopathic phenotype was further illustrated by a significant increase in heart weight-to-tibia length and lung

weight-to-tibia length ratios in both 4-5 month-old DMPK E line 1 and 8-10 month-old DMPK E line 2 transgenic mice, compared to 8-10 month-old WT mice (Fig. 7E and F). This increase in heart and lung weights was not observed in 8-10 month-old DMPK E (K100A) mice (Fig. 7E and F). So, an increase in DMPK E kinase activity in postnatal hearts results in cardiomyopathy and death.

To obtain more mechanistic insight in the DMPK E induced cardiomyopathy, we sacrificed mice at 10 weeks of age and performed electron microscopy on cardiac tissue (Fig. 7G and H and Fig. S5C). Quantification of sarcomere structure score indicated that sarcomere structure is severely disrupted in DMPK E transgenic mice (Fig. 7H). Staining of cardiac sections for α -actinin further verified a loss of sarcomere structure in DMPK E mice compared to both WT and DMPK E (K100A) mice (Fig. 7I).

Furthermore, immunostaining for SRF revealed a significant decrease in cardiomyocytes with an SRF positive nucleus in DMPK E mice compared to WT and DMPK E (K100A) mice (Fig. 7I and J). In line, QPCR for SRF-regulated sarcomeric genes revealed a significant decrease of Ttn, Actn2 and Myl2 expression in DMPK E mice, compared to both WT and DMPK E (K100A) control mice (Fig. 7K). In contrast to our observations in NRCM (Fig. 5A), Acta1 mRNA levels were significantly higher in DMPK E hearts (Fig. 7K), which could be due to the reactivation of the fetal gene program during cardiac stress. Overall, an increase in DMPK E kinase activity in the heart results in cardiomyopathy. This cardiomyopathy is preceded by a loss of sarcomere structure and inhibition of SRF transcriptional activity.

DISCUSSION

Ultrastructural changes in cardiomyocytes are characteristic features of heart failure development and disruption of sarcomeres is found to be an early predictor of prognosis in

dilated cardiomyopathy patients²⁵. Previous work has demonstrated the contribution of MEF2 to structural remodeling of cardiomyocytes in heart failure progression^{4, 5, 11}, but the underlying mechanism and responsible MEF2 transcriptional targets are unknown. In present study, we confirmed the importance of MEF2 in adverse cardiomyocyte remodeling, since MEF2 activation induced elongation of cardiomyocytes and loss of sarcomere components at both the M-band and Z-disc. Concordantly, the classification profile of MEF2 target genes we identified revealed an intimate involvement of MEF2 in regulation of cellular structure.

We identified DMPK as direct transcriptional target of MEF2 with a crucial role in disruption of sarcomere structure (Fig. S7). DMPK did not seem to affect cardiomyocyte length, indicating that the MEF2-induced cardiomyocyte elongation involves other MEF2 transcriptional targets. DMPK protein levels are found to be increased in human failing hearts¹⁸, but DMPK is mainly known from its implication in myotonic dystrophy 1 (DM1). DM1 is an inherited multisystemic neuromuscular disorder and symptoms include progressive muscle weakness and wasting, cataracts, gastro-intestinal problems and cardiac abnormalities²⁶. DM1 has been associated with expansion of untranslated CTG repeats in the 3'-untranslated region of *DMPK*, which causes accumulation of DMPK mRNA transcripts in the nucleus, resulting in RNA toxicity and *trans* effects altering expression and alternative splicing of numerous other genes^{27, 28}. It is unclear, however, whether these *trans* RNA processing defects are solely responsible for the DM1 cardiac pathology, since altered DMPK levels are by itself sufficient to induce cardiac defects similar to those observed in DM1 patients^{29, 30}. Nevertheless, most studies on DM1 focus on the pathological effects associated with the untranslated CTG expansion, leaving a functional role for DMPK largely unexplored.

Findings in several other studies underline the potential role for DMPK in cardiomyocyte remodeling. DMPK is related to the Rho family of protein kinases, which are associated with actin cytoskeletal remodeling³¹. DMPK is also known to interact with Rac-1, and both DMPK and Rac-1 are able to phosphorylate and inhibit myosin phosphatase^{32, 33}. Inhibition of myosin

phosphatase and associated increase in myosin phosphorylation is important for sarcomere organization³⁴. Also, overexpression of DMPK in chick cardiomyocytes leads to disruption of sarcomeres¹⁶. Finally, Mulders *et al.* have demonstrated that overexpression of DMPK E, but not the longer DMPK C isoform, hampers sarcomere assembly during differentiation of skeletal muscle cells¹⁷. Their results suggest that the effects of DMPK E on sarcomere structure mainly involve a disturbance in sarcomere formation instead of active breakdown of sarcomere components, which is in agreement with our findings that DMPK E inhibits sarcomeric gene expression. A recent report by Carell *et al.*³⁵ suggests that targeting all DMPK isoforms in mice is not sufficient to prevent loss of cardiac function after induction of pressure overload. In their study, however, they only investigated the effect of DMPK inhibition during early cardiac remodeling and not in end-stage heart failure, when DMPK E is upregulated and a disturbance in sarcomere formation is expected.

The absence of any morphological or functional changes after overexpression of the kinase dead DMPK mutant in both our *in vitro* and *in vivo* experiments indicates the requirement of DMPK enzymatic activity and one or more downstream phosphorylation targets in the cellular remodeling process. Besides myosin phosphatase, DMPK is known to phosphorylate a small set of other targets, including phospholamban³⁶, phospholemman³⁷, CUG-binding protein³⁸ and SRF²¹. Like MEF2, SRF is a MADS box containing transcription factor essential for cardiac differentiation. SRF binds to a DNA consensus element known as CArG box, which is primarily found in promoters of genes involved in cell growth, cell movement and contractility²⁴. The importance of SRF in the heart is illustrated by several studies in mouse models, which demonstrate that SRF loss of function results in dilated cardiomyopathy and death associated with decreased levels of sarcomeric proteins⁹.

DMPK has been found to phosphorylate SRF at serines 159 and 162 in the DNA binding MADS box domain²¹. This phosphorylation event has initially been described to activate transcription of skeletal alpha-actin²¹. Later, however, phosphorylation of serine 162 was

described to prevent SRF binding to CArG boxes in DNA, allowing this phosphorylation event to act as a switch between myogenic and proliferation gene programs²³. Our findings are in agreement with loss of SRF-DNA binding, since we observed a reduction in SRF transcriptional activity in association with translocation of SRF out of the nucleus. A redistribution of SRF from the nucleus to the cytosol has been described earlier as mechanism to inhibit SRF transcriptional regulation of contractile genes in serum deprived smooth muscle cells³⁹. Interestingly, this translocation of SRF was controlled by the Rho kinase pathway⁴⁰. Cytoplasmic accumulation of SRF has also been observed in NRCM after mechanical arrest⁴¹.

In conclusion, our findings identify DMPK as a direct transcriptional target of MEF2, promoting sarcomere degeneration, a main characteristic of cardiomyocytes during heart failure progression. The loss of sarcomere structure is caused by a reduction of sarcomeric gene transcription, which is, at least in part, due to inhibition of SRF transcriptional activity.

FUNDING

This work was supported by the Medical Research Council and the British Heart Foundation [E.E.]; the *Netherlands CardioVascular Research Initiative*: the Dutch Heart Foundation, Dutch Federation of University Medical Centers, the Netherlands Organization for Health Research and Development (ZonMW) and the Royal Netherlands Academy of Sciences [L.D.W. and Y.M.P.]; the European Research Council (ERC) [311549 to L.D.W.]; the Netherlands Organization for Scientific Research (NWO) [918.156.47 to L.D.W., 916.11.150 to R.J.v.O.]; and the Dutch Heart Foundation (NHS) [2012T094 to R.J.v.O.].

ACKNOWLEDGEMENTS

The authors are grateful to Dr. Eric Olson for providing NkL-TAg cells and to Dr. Thomas Cooper and Dr. Esther Creemers for sharing plasmids. The authors also thank Nina de Groot for technical assistance and Dr. Jan M. Ruijter for helpful discussion.

CONFLICT OF INTEREST

None declared.

REFERENCES

1. Gerdes AM, Capasso JM. Structural remodeling and mechanical dysfunction of cardiac myocytes in heart failure. *J Mol Cell Cardiol* 1995;**27**:849-856.
2. Schaper J, Froede R, Hein S, Buck A, Hashizume H, Speiser B, Friedl A, Bleese N. Impairment of the myocardial ultrastructure and changes of the cytoskeleton in dilated cardiomyopathy. *Circulation* 1991;**83**:504-514.
3. Hein S, Scholz D, Fujitani N, Renollet H, Brand T, Friedl A, Schaper J. Altered expression of titin and contractile proteins in failing human myocardium. *J Mol Cell Cardiol* 1994;**26**:1291-1306.
4. van Oort RJ, van Rooij E, Bourajjaj M, Schimmel J, Jansen MA, van der Nagel R, Doevendans PA, Schneider MD, van Echteld CJ, De Windt LJ. MEF2 activates a genetic program promoting chamber dilation and contractile dysfunction in calcineurin-induced heart failure. *Circulation* 2006;**114**:298-308.

5. Xu J, Gong NL, Bodi I, Aronow BJ, Backx PH, Molkentin JD. Myocyte enhancer factors 2A and 2C induce dilated cardiomyopathy in transgenic mice. *J Biol Chem* 2006;**281**:9152-9162.
6. Gossett LA, Kelvin DJ, Sternberg EA, Olson EN. A new myocyte-specific enhancer-binding factor that recognizes a conserved element associated with multiple muscle-specific genes. *Mol Cell Biol* 1989;**9**:5022-5033.
7. Black BL, Olson EN. Transcriptional control of muscle development by myocyte enhancer factor-2 (MEF2) proteins. *Annu Rev Cell Dev Biol* 1998;**14**:167-196.
8. McKinsey TA, Zhang CL, Olson EN. MEF2: a calcium-dependent regulator of cell division, differentiation and death. *Trends Biochem Sci* 2002;**27**:40-47.
9. Dirx E, da Costa Martins PA, De Windt LJ. Regulation of fetal gene expression in heart failure. *Biochim Biophys Acta* 2013;**1832**:2414-2424.
10. Heineke J, Molkentin JD. Regulation of cardiac hypertrophy by intracellular signalling pathways. *Nat Rev Mol Cell Biol* 2006;**7**:589-600.
11. Kim Y, Phan D, van Rooij E, Wang DZ, McAnally J, Qi X, Richardson JA, Hill JA, Bassel-Duby R, Olson EN. The MEF2D transcription factor mediates stress-dependent cardiac remodeling in mice. *J Clin Invest* 2008;**118**:124-132.
12. el Azzouzi H, van Oort RJ, van der Nagel R, Sluiter W, Bergmann MW, De Windt LJ. MEF2 transcriptional activity maintains mitochondrial adaptation in cardiac pressure overload. *Eur J Heart Fail* 2010;**12**:4-12.
13. Rybkin, II, Markham DW, Yan Z, Bassel-Duby R, Williams RS, Olson EN. Conditional expression of SV40 T-antigen in mouse cardiomyocytes facilitates an inducible switch from proliferation to differentiation. *J Biol Chem* 2003;**278**:15927-15934.
14. Czubryt MP, McAnally J, Fishman GI, Olson EN. Regulation of peroxisome proliferator-activated receptor gamma coactivator 1 alpha (PGC-1 alpha) and mitochondrial function by MEF2 and HDAC5. *Proc Natl Acad Sci U S A* 2003;**100**:1711-1716.

15. Naya FJ, Black BL, Wu H, Bassel-Duby R, Richardson JA, Hill JA, Olson EN. Mitochondrial deficiency and cardiac sudden death in mice lacking the MEF2A transcription factor. *Nat Med* 2002;**8**:1303-1309.
16. Harmon EB, Harmon ML, Larsen TD, Paulson AF, Perryman MB. Myotonic dystrophy protein kinase is expressed in embryonic myocytes and is required for myotube formation. *Dev Dyn* 2008;**237**:2353-2366.
17. Mulders SA, van Horssen R, Gerrits L, Bennink MB, Pluk H, de Boer-van Huizen RT, Croes HJ, Wijers M, van de Loo FA, Fransen J, Wieringa B, Wansink DG. Abnormal actomyosin assembly in proliferating and differentiating myoblasts upon expression of a cytosolic DMPK isoform. *Biochim Biophys Acta* 2011;**1813**:867-877.
18. Vitello AM, Du Y, Buttrick PM, Walker LA. Serendipitous discovery of a novel protein signaling mechanism in heart failure. *Biochem Biophys Res Commun* 2012;**421**:431-435.
19. Groenen PJ, Wansink DG, Coerwinkel M, van den Broek W, Jansen G, Wieringa B. Constitutive and regulated modes of splicing produce six major myotonic dystrophy protein kinase (DMPK) isoforms with distinct properties. *Hum Mol Genet* 2000;**9**:605-616.
20. Wansink DG, van Herpen RE, Coerwinkel-Driessen MM, Groenen PJ, Hemmings BA, Wieringa B. Alternative splicing controls myotonic dystrophy protein kinase structure, enzymatic activity, and subcellular localization. *Mol Cell Biol* 2003;**23**:5489-5501.
21. Iyer D, Belaguli N, Fluck M, Rowan BG, Wei L, Weigel NL, Booth FW, Epstein HF, Schwartz RJ, Balasubramanyam A. Novel phosphorylation target in the serum response factor MADS box regulates alpha-actin transcription. *Biochemistry* 2003;**42**:7477-7486.
22. Creemers EE, Sutherland LB, Oh J, Barbosa AC, Olson EN. Coactivation of MEF2 by the SAP domain proteins myocardin and MASTR. *Mol Cell* 2006;**23**:83-96.
23. Iyer D, Chang D, Marx J, Wei L, Olson EN, Parmacek MS, Balasubramanyam A, Schwartz RJ. Serum response factor MADS box serine-162 phosphorylation switches

- proliferation and myogenic gene programs. *Proc Natl Acad Sci U S A* 2006;**103**:4516-4521.
24. Niu Z, Li A, Zhang SX, Schwartz RJ. Serum response factor micromanaging cardiogenesis. *Curr Opin Cell Biol* 2007;**19**:618-627.
 25. Saito T, Asai K, Sato S, Takano H, Mizuno K, Shimizu W. Ultrastructural features of cardiomyocytes in dilated cardiomyopathy with initially decompensated heart failure as a predictor of prognosis. *Eur Heart J* 2015;**36**:724-732.
 26. Hermans MC, Faber CG, Bekkers SC, de Die-Smulders CE, Gerrits MM, Merkies IS, Snoep G, Pinto YM, Schalla S. Structural and functional cardiac changes in myotonic dystrophy type 1: a cardiovascular magnetic resonance study. *J Cardiovasc Magn Reson* 2012;**14**:48.
 27. Mahadevan M, Tsilfidis C, Sabourin L, Shutler G, Amemiya C, Jansen G, Neville C, Narang M, Barcelo J, O'Hoy K, et al. Myotonic dystrophy mutation: an unstable CTG repeat in the 3' untranslated region of the gene. *Science* 1992;**255**:1253-1255.
 28. Pettersson OJ, Aagaard L, Jensen TG, Damgaard CK. Molecular mechanisms in DM1 - a focus on foci. *Nucleic Acids Res* 2015;**43**:2433-2441.
 29. Berul CI, Maguire CT, Aronovitz MJ, Greenwood J, Miller C, Gehrman J, Housman D, Mendelsohn ME, Reddy S. DMPK dosage alterations result in atrioventricular conduction abnormalities in a mouse myotonic dystrophy model. *J Clin Invest* 1999;**103**:R1-7.
 30. O'Coilain DF, Perez-Terzic C, Reyes S, Kane GC, Behfar A, Hodgson DM, Strommen JA, Liu XK, van den Broek W, Wansink DG, Wieringa B, Terzic A. Transgenic overexpression of human DMPK accumulates into hypertrophic cardiomyopathy, myotonic myopathy and hypotension traits of myotonic dystrophy. *Hum Mol Genet* 2004;**13**:2505-2518.
 31. Amano M, Fukata Y, Kaibuchi K. Regulation and functions of Rho-associated kinase. *Exp Cell Res* 2000;**261**:44-51.

32. Muranyi A, Zhang R, Liu F, Hirano K, Ito M, Epstein HF, Hartshorne DJ. Myotonic dystrophy protein kinase phosphorylates the myosin phosphatase targeting subunit and inhibits myosin phosphatase activity. *FEBS Lett* 2001;**493**:80-84.
33. Shimizu M, Wang W, Walch ET, Dunne PW, Epstein HF. Rac-1 and Raf-1 kinases, components of distinct signaling pathways, activate myotonic dystrophy protein kinase. *FEBS Lett* 2000;**475**:273-277.
34. Aoki H, Sadoshima J, Izumo S. Myosin light chain kinase mediates sarcomere organization during cardiac hypertrophy in vitro. *Nat Med* 2000;**6**:183-188.
35. Carrell ST, Carrell EM, Auerbach D, Pandey SK, Bennett CF, Dirksen RT, Thornton CA. Dmpk gene deletion or antisense knockdown does not compromise cardiac or skeletal muscle function in mice. *Hum Mol Genet* 2016;**25**:4328-4338.
36. Kaliman P, Catalucci D, Lam JT, Kondo R, Gutierrez JC, Reddy S, Palacin M, Zorzano A, Chien KR, Ruiz-Lozano P. Myotonic dystrophy protein kinase phosphorylates phospholamban and regulates calcium uptake in cardiomyocyte sarcoplasmic reticulum. *J Biol Chem* 2005;**280**:8016-8021.
37. Mounsey JP, John JE, 3rd, Helmke SM, Bush EW, Gilbert J, Roses AD, Perryman MB, Jones LR, Moorman JR. Phospholemman is a substrate for myotonic dystrophy protein kinase. *J Biol Chem* 2000;**275**:23362-23367.
38. Roberts R, Timchenko NA, Miller JW, Reddy S, Caskey CT, Swanson MS, Timchenko LT. Altered phosphorylation and intracellular distribution of a (CUG)_n triplet repeat RNA-binding protein in patients with myotonic dystrophy and in myotonin protein kinase knockout mice. *Proc Natl Acad Sci U S A* 1997;**94**:13221-13226.
39. Camoretti-Mercado B, Liu HW, Halayko AJ, Forsythe SM, Kyle JW, Li B, Fu Y, McConville J, Kogut P, Vieira JE, Patel NM, Hershenson MB, Fuchs E, Sinha S, Miano JM, Parmacek MS, Burkhardt JK, Solway J. Physiological control of smooth muscle-

specific gene expression through regulated nuclear translocation of serum response factor. *J Biol Chem* 2000;**275**:30387-30393.

40. Liu HW, Halayko AJ, Fernandes DJ, Harmon GS, McCauley JA, Kocieniewski P, McConville J, Fu Y, Forsythe SM, Kogut P, Bellam S, Dowell M, Churchill J, Lesso H, Kassiri K, Mitchell RW, Hershenson MB, Camoretti-Mercado B, Solway J. The RhoA/Rho kinase pathway regulates nuclear localization of serum response factor. *Am J Respir Cell Mol Biol* 2003;**29**:39-47.
41. Lange S, Xiang F, Yakovenko A, Vihola A, Hackman P, Rostkova E, Kristensen J, Brandmeier B, Franzen G, Hedberg B, Gunnarsson LG, Hughes SM, Marchand S, Sejersen T, Richard I, Edstrom L, Ehler E, Udd B, Gautel M. The kinase domain of titin controls muscle gene expression and protein turnover. *Science* 2005;**308**:1599-1603.

FIGURE LEGENDS

Figure 1. MEF2 activation induces cardiomyocyte elongation and loss of sarcomeres.

A. Confocal immunocytochemistry of NRCM after adenoviral overexpression of either GFP, MEF2A or constitutively active MEF2 (caMEF2) using antibodies raised against titin epitopes located in the Z-disc (titin T12) and in the M-band (titin M8). Scale bar = 10 μ m. **B.** Confocal immunocytochemistry of NRCM after adenoviral overexpression of either GFP, MEF2A or caMEF2 using anti-sarcomeric α -actinin (Z-disc) and anti-myomesin (M-band). Scale bar = 10 μ m. **C.** Quantitative examination of cell-length/cell-width ratios of cardiomyocytes from 3 independent isolations infected with AdGFP (n=102 cells), AdMEF2A (n=101 cells) and AdcaMEF2 (n=100 cells). ***P<0.001 versus AdGFP, ##P<0.05 versus AdMEF2A, one way ANOVA followed by Tukey's post-test. **D.** Quantification of the myofibrillar structure in NRCM from 4 independent isolations transduced with either AdGFP (n=190 cells), AdMEF2A (n=280 cells), or AdcaMEF2 (n=192 cells). ***P<0.001 versus AdGFP, #P<0.05 versus AdMEF2A, one way ANOVA followed by Tukey's post-test.

Figure 2. Characterization of MEF2 target genes in cardiac cell lines inducibly expressing caMEF2.

A. Schematic representation of a double-stable cardiomyocyte cell line harboring a construct expressing Tet repressor (TR) and a construct harboring caMEF2 downstream of Tet operators (tetO), which expresses caMEF2 only after doxycycline (Dox) stimulation. **B.** Luciferase measurements on TR1-194 and TR4-39 cells, transiently transfected with a MEF2 luciferase reporter, indicating an increase in MEF2 activity after Dox stimulation. n=3 replicates. **C.** Bar graph indicating the number of genes identified by microarray analysis to be differentially expressed in both TR1-194 and TR4-39 cells in different functional classifications. **D.** RT-PCR validation of mRNA levels of indicated genes in TR1-194 and TR4-39 cells in absence or

presence of Dox. Ribosomal protein L7 mRNA levels were determined as control for equal loading and amplification. **E.** QPCR analysis of indicated genes in TR4-39 cells in absence or presence of Dox. n=4 replicates. *P<0.05, **P<0.01 and ***P<0.001 versus -Dox. One way ANOVA followed by Tukey's post-test.

Figure 3. DMPK is a transcriptional target of MEF2 promoting sarcomere degeneration.

A. Sequence alignment of rat, mouse, and human *dmpk* promoter regions. The gray box indicates a conserved MEF2 binding site. **B.** Chromatin immunoprecipitation (ChIP) analysis performed by PCR using primers flanking the MEF2 site on DNA immunoprecipitated using either a MEF2 or an acetylated histone H3 antibody. Non-immunoprecipitated DNA was used as input control. **C.** Western blot analysis for DMPK expression in NRCM pre-transfected with control or DMPK specific siRNAs and infected with indicated adenoviruses. Immunoreactivity for GAPDH serves as protein loading control. **D.** Confocal immunocytochemistry of NRCM, using an α -actinin antibody, demonstrates that knockdown of DMPK attenuates MEF2 induced sarcomere degeneration. Experiment has been repeated 3 times and representative images are shown. Scale bar = 20 μ m.

Figure 4. Expression of DMPK E is increased in failing mouse hearts and is sufficient to disrupt sarcomeric organization.

A. Western blot analysis for DMPK expression in control, failing and hypertrophic mouse hearts after TAC, displaying increased DMPK expression only in failing hearts. **B.** Quantification of DMPK protein expression in 6 sham, 4 failing and 4 hypertrophied mice, demonstrating a significant increase of DMPK expression in failing, but not hypertrophic mouse hearts. * P<0.05 vs. sham, one way ANOVA followed by Tukey's post-test. **C.** RT-PCR analysis for different DMPK splice variants in healthy and failing hearts from mice subjected to sham or TAC surgery. Exons 13 and 14 skip is DMPK E. **D.** QPCR analysis demonstrates a significant increase in

expression of the DMPK E isoform in failing mouse hearts. n=9 control mice and 8 heart failure mice. *P<0.05, unpaired 2-tailed Student's t-test. **E.** Western blot analysis demonstrating adenoviral expression of DMPK E and a kinase dead mutant DMPK E (K100A). **F.** Quantification of the myofibrillar structure in NRCM from 3 independent isolations transduced with either AdGFP (n=66 cells), AdDMPK E (n=62 cells), or AdDMPK E (K100A) (n=69 cells). ***P<0.001 versus AdGFP, ####P<0.001 versus AdDMPK E, one way ANOVA followed by Tukey's post-test. **G.** Representative confocal images of NRCM transduced with AdGFP, AdDMPK E, or AdDMPK E (K100A). Scale bar = 20 μ m.

Figure 5. DMPK E decreases expression of sarcomeric genes and inhibits SRF transcriptional activity.

A. QPCR analysis indicates a decrease in mRNA levels of sarcomeric genes after DMPK E overexpression in NRCM. n=3. *P<0.05, ***P<0.001 versus AdGFP, one way ANOVA followed by Tukey's post-test. **B.** Luciferase experiment using SM22-luc reporter in NRCM indicates that DMPK E inhibits SRF transcriptional activity. n=4 replicates. *P<0.05, ***P<0.001 versus AdGFP, one way ANOVA followed by Tukey's post-test. **C and D.** Confocal immunocytochemistry on NRCM for α -actinin and SRF displays translocation of SRF out of the nucleus in cardiomyocytes expressing DMPK E (**D**). Quantification of the ratio of nuclear versus cytoplasmic SRF in NRCM transduced with AdGFP, AdDMPK E and AdDMPK E (K100A) showing less nuclear SRF in cells overexpressing DMPK E (**C**). AdGFP: n=54 cells, AdDMPK E: n=56 cells, AdDMPK E (K100A): n=51 cells from 3 independent cell isolations. ***P<0.001 versus AdGFP, ####P<0.001 versus AdDMPK E, one way ANOVA followed by Tukey's post-test. Scale bar = 20 μ m.

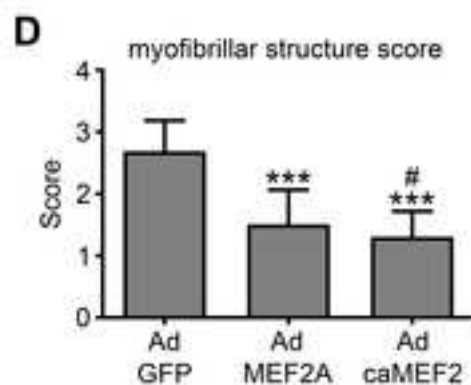
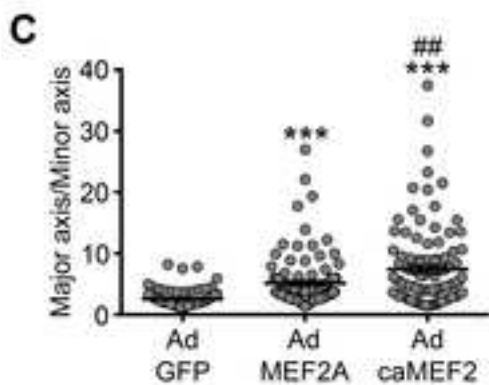
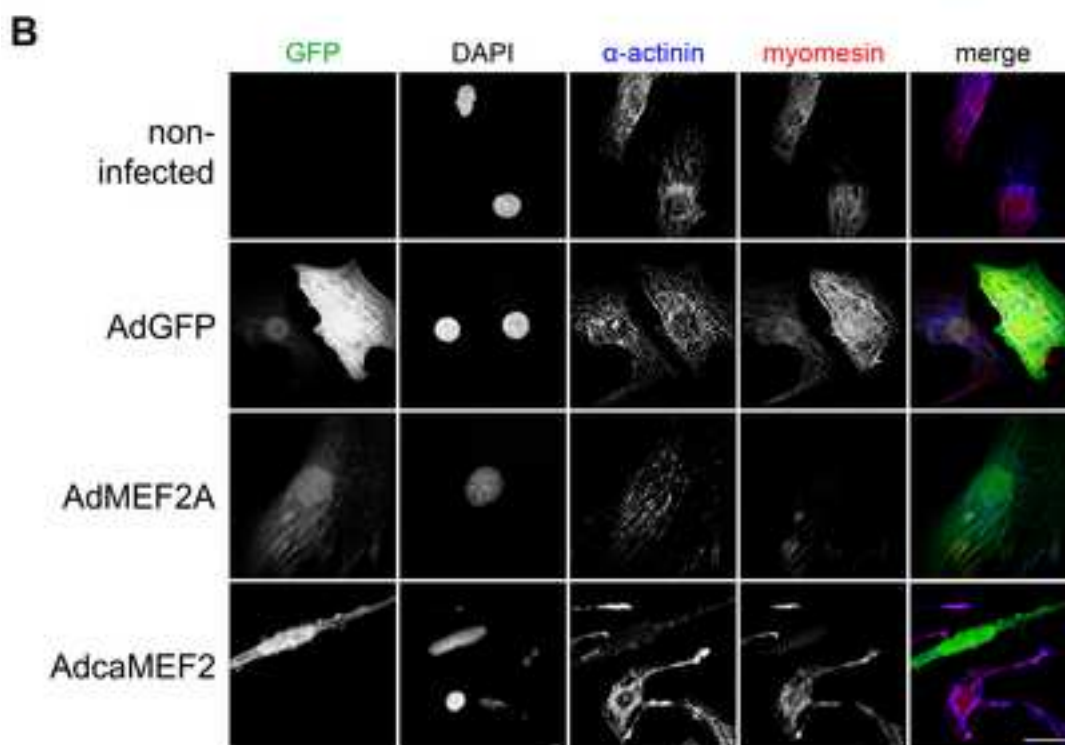
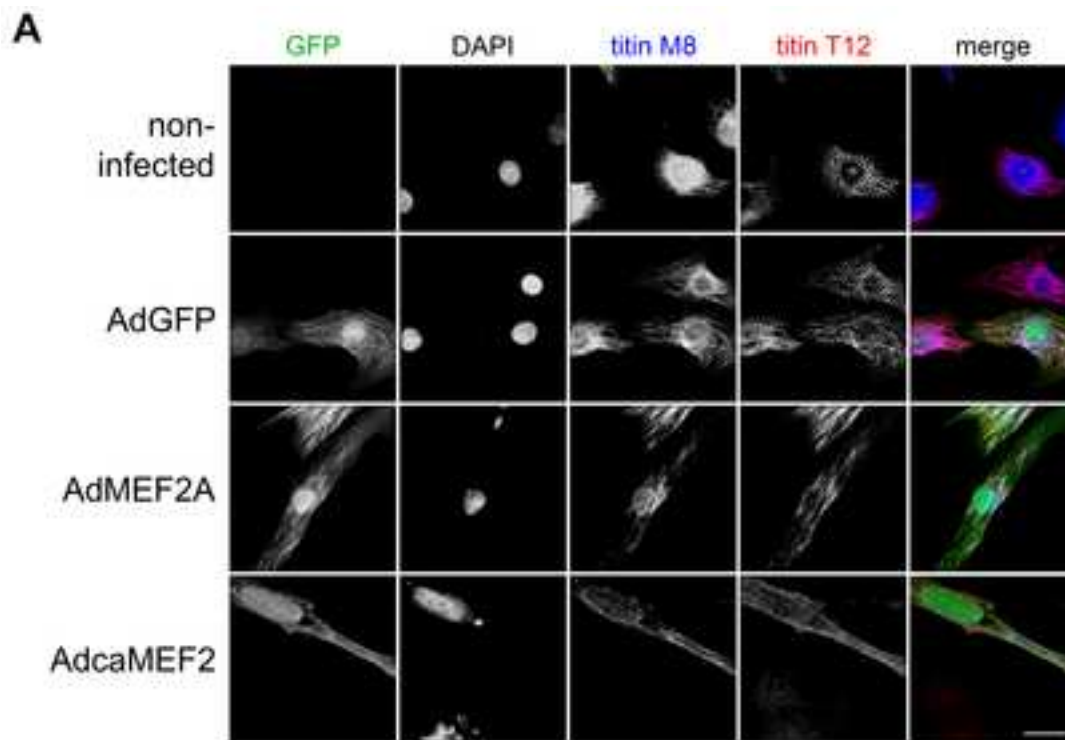
Figure 6. DMPK E-induced loss of sarcomere structure requires phosphorylation of SRF.

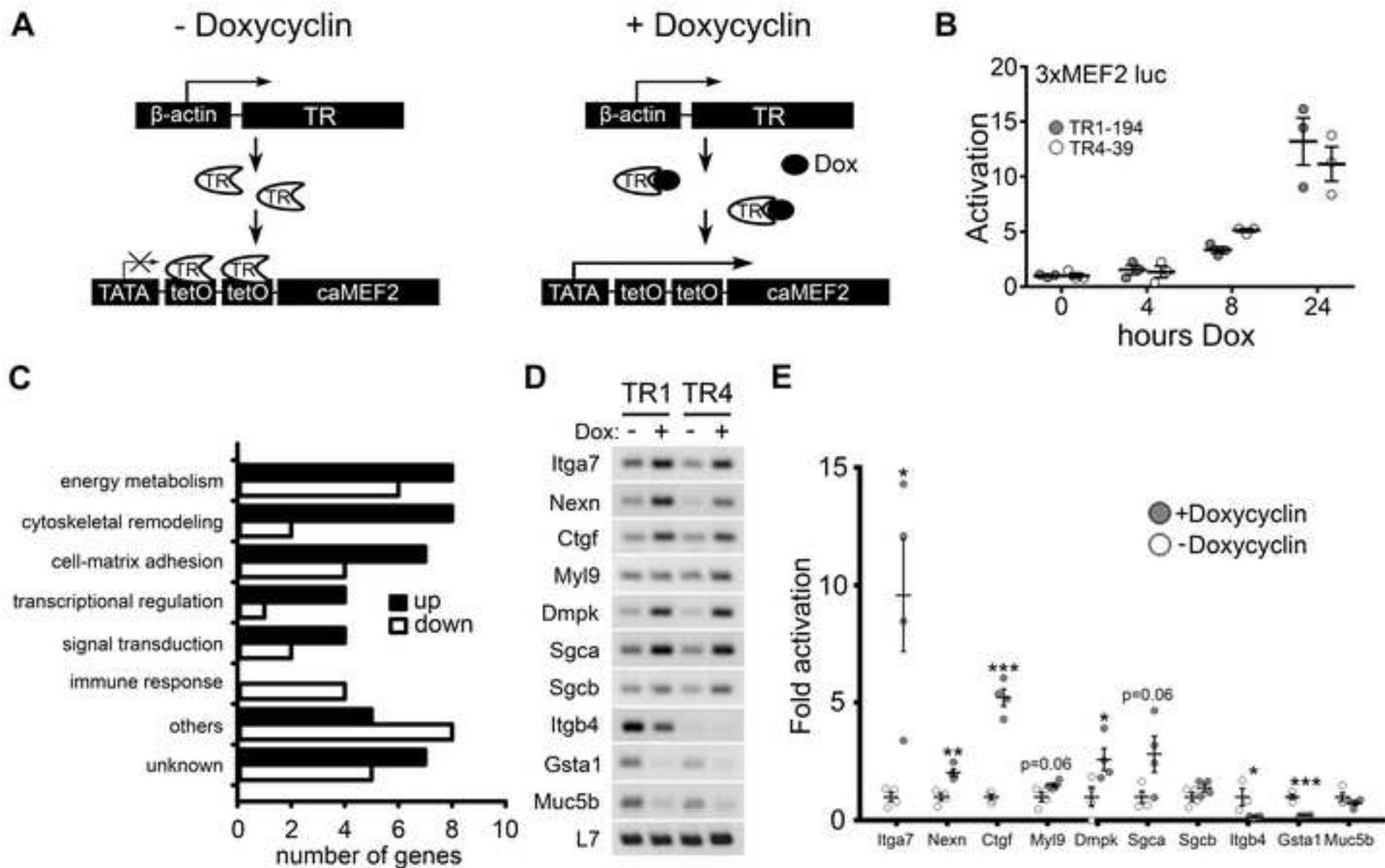
A. Confocal immunocytochemistry on NRCM co-transduced with either AdGFP or AdDMPK E, and lenti-SRF-WT (wildtype SRF), lenti-SRF-TASA (unphosphorylatable mutant) or lenti-SRF-TDSD (phosphomimic), where the three SRF constructs are tagged with a red fluorescent protein (RFP). **B.** Quantification of the nuclear localization of SRF-WT, SRF-TASA and SRF-TDSD in NRCM transduced with AdGFP or AdDMPK E. n=33 cells from 3 independent cell isolations. ***P<0.001, ###P<0.001 versus corresponding WT, one way ANOVA followed by Tukey's post-test. **C.** Confocal immunocytochemistry on NRCM transduced with AdDMPK E with or without lenti-SRF-TASA. **D.** Quantification of the myofibrillar structure in NRCM transduced with AdDMPK E with or without SRF-TASA, showing improvement of the sarcomere structure upon SRF-TASA expression. AdDMPK E: n=102 cells, AdDMPK E/SRF-TASA: n=53 cells, from 3 independent isolations. ***P<0.001 versus AdDMPK E, one way ANOVA followed by Tukey's post-test. Scale bar = 20 μ m.

Figure 7. Cardiac specific overexpression of DMPK E induces loss of sarcomeric structure and cardiomyopathy.

A. Western blot for DMPK on cardiac lysates from mice from two independent DMPK E and two DMPK E (K100A) transgenic lines. Note the absence of DMPK autophosphorylation product (higher protein band) in DMPK E (K100A) mice. **B.** QPCR analysis showing DMPK E mRNA expression in WT (n=10), DMPK E lines 1 (n=3) and 2 (n=4), and in DMPK E (K100A) lines 1 (n=3) and 2 (n=5) hearts. *** P<0.001 versus all transgenic lines, P<0.05, ## P<0.01 vs DMPK E line 1, one way ANOVA followed by Tukey's post-test. **C.** Kaplan-Meier curve revealing increased mortality in DMPK E compared to WT and DMPK E (K100A) transgenic mice. WT: n=38, DMPK E line 1: n=29, DMPK E line 2: n=27, DMPK E (K100A) line 1: n=26, DMPK E (K100A) line 2: n=24. **D.** Representative images of whole hearts and H&E stained sections from 8 months old WT and transgenic mice and a 5 months old DMPK E line 1 transgenic mouse, displaying cardiomyopathy after overexpression of DMPK E, but not DMPK E (K100A). **E, F.** Dot

plots indicating an increase in heart weight-to-tibia length (HW/TL) (**E**) and lung weight-to-tibia length (LuW/TL) (**F**) in DMPK E transgenic mice (line 1: 4-5 months old, n=6; line 2: 8-10 months old, n=8) compared to 8-10 months old WT (n=8) and DMPK E (K100A) transgenic mice (line 1: n=10; line 2: n=6). *P<0.05, **P<0.01, ***P<0.001 vs WT; #P<0.05, ##P<0.01, ###P<0.001 vs DMPK E line 1; \$P<0.05 vs DMPK E line 2, one way ANOVA followed by Tukey's post-test. **G.** Electron microscopy images of hearts of 10 week old WT, DMPK E and DMPK E (K100A) mice displaying heavily disorganized sarcomeres in DMPK E hearts. Scale bar = 5 μ m. **H.** Quantification of EM sarcomere structure score. WT (n=155 EM pictures), DMPK E line 1 (n=155 EM pictures), DMPK E (K100A) line 1 (n=102 EM pictures) from 3 to 4 mice per group. ***P<0.001 vs WT, ###P<0.001 vs DMPK E, one way ANOVA followed by Tukey's post-test. **I.** Confocal images of cardiac sections from 10 week old mice, stained for α -actinin (green), SRF (red) and DAPI (blue), demonstrating a loss of sarcomere organization in DMPK E transgenic hearts. Scale bar = 20 μ m. **J.** Quantification of cardiomyocytes with SRF positive nuclei, showing a decrease in number of SRF positive cardiomyocytes in DMPK E transgenic mice compared to WT and DMPK E (K100A) transgenic controls (10 weeks old, n=4 for all groups). ***P<0.001 vs WT, ###P<0.001 vs DMPK E, one way ANOVA followed by Tukey's post-test. **K.** QPCR analysis of SRF-regulated sarcomeric genes in WT (Ttn: n=4, Actn2: n=4, Myl2: n=4, Acta1: n= 5), DMPK E (Ttn: n=5, Actn2: n=4, Myl2: n=6, Acta1: n=4) and DMPK E (K100A) (Ttn: n=3, Actn2: n=3, Myl2: n=4, Acta1: n=4) transgenic mice. *P<0.05, **P<0.01, ***P<0.001 vs WT; #P<0.05, ##P<0.01, ###P<0.001 vs DMPK E, one way ANOVA followed by Tukey's post-test.





A

```

rat      TCGTC-----TACCTTCTGCCAAAGG-----GGGGTGGGGGTA--ATA
mouse   TCTTCCTT---CTACCTCCTGCCAAAAAAT-----GGGGGGGGGGTA--ATA
human   CCACCCCTTCCCCACCTCCTGGGAAAAAAAAAAAAAAAAAAAAAGCTGGTATAAG
      * *          **** * * * *          * * * * *

rat      CAGCAGGCCCAGGGGCTAAATTTAACTGTCCCAAAGTGGGAATCCATTGCTGAGTCACG-
mouse   CAGCAGGCCACAGGGGCTAAATTTAACTGTCCCAAAGTCGGAATCCATTGCTGAGTCACG-
human   CAGAGAGCCTGAGGGCTAAATTTAACTGTCC--GAGTCGGAATCCATCTCTGAGTCAACC
      *** **          *****          *** ***** *****

rat      AAGAAGCTGCCCTGGTCCC GGCCCCCTC-----CCCTGTAGGCCCAGGC
mouse   AAGAAGCTGCCCTGGCCTTTGGCCCCCCCCACTACCCCTCACCCCTGTGTG-CCCAGGC
human   AAGAAGCTGCCCTGGCCTCCCGTCCCCTTCCAGGCCTCAACCCCTTTCTCCACCCAGC
      ***** *          *****          * * * * * ** **

```

